Am J Transl Res 2026;18(4):3509-3512
www.ajtr.org /ISSN:1943-8141/AJTR0171368

Case Report

Infantile hypophosphatasia caused by compound heterozygous variants in the *ALPL* gene: a case report

Qian Wu, Min Xiang, Wei Xiong, Bangzhen Wang, Sha Wu, Maoqiong Chen

Department of Neonatology, Affiliated Hospital of Guizhou Medical University/Guizhou Hospital, First Affiliated Hospital of Sun Yat-Sen University, Guiyang 550000, Guizhou, China

Received January 10, 2026; Accepted March 25, 2026; Epub April 25, 2026; Published April 30, 2026

Abstract: This article reports a case of infantile hypophosphatasia (HPP) due to compound heterozygous *alkaline phosphatase-liver/bone/kidney* (*ALPL*) gene mutations, and analyzes its clinical phenotype and genetic characteristics. A retrospective analysis was conducted on the clinical data, genetic testing results, and family history of a male infant with HPP. The infant presented with intrauterine and postpartum growth retardation, respiratory failure, feeding difficulties, vitamin B6-responsive epileptic seizures, bone hypomineralization, hypercalcemia, and very low alkaline phosphatase (ALP). Genetic testing revealed compound heterozygous *ALPL* mutations: c.533A>G (p.Tyr178Cys) and c.644T>A (p.Ile215Asn), inherited from his father and mother, respectively, both parents being phenotypically normal. The mother had previously terminated a pregnancy due to fetal bone deformity. This case of infantile HPP resulted from compound heterozygous *ALPL* mutations, with typical clinical features including bone hypomineralization, hypercalcemia, and profoundly low ALP. Without enzyme replacement therapy, the disease is progressing.

Keywords: Infantile hypophosphatasia, *ALPL* gene, enzyme replacement therapy, case report

Introduction

Hypophosphatasia (HPP) is a rare hereditary metabolic bone disorder resulting from pathogenic variants in the *alkaline phosphatase-liver/bone/kidney* (*ALPL*) gene encoding tissue-nonspecific alkaline phosphatase (TNSALP) [1]. Loss-of-function mutations reduce TNSALP activity, impairing bone mineralization [2]. This disease exhibits significant clinical heterogeneity, classified into six subtypes based on onset age and severity. Perinatal lethal and infantile subtypes, characterized by early onset and rapid progression, are associated with high mortality and termed severe HPP [3]. Clinical features include severe bone hypomineralization, respiratory insufficiency, refractory hypercalcemia, and vitamin B6-dependent seizures [4].

Severe HPP typically follows autosomal recessive inheritance, with homozygous or compound heterozygous *ALPL* mutations markedly reducing or eliminating TNSALP activity [5]. Epidemiologic data from China are limited, with only sporadic case reports published. Prenatal ultrasound features of severe HPP may resemble other lethal skeletal dysplasias, often causing diagnostic delay [6]. This report presents the clinical and genetic findings of an infantile HPP case caused by compound heterozygous *ALPL* mutations to enhance clinical awareness.

Patient and methods

Subject

We retrospectively analyzed a patient diagnosed with infantile HPP at the Affiliated Hospital of Guizhou Medical University in 2025. Clinical data, family history, laboratory, imaging, and genetic testing results were collected. The study was approved by the Ethics Committee of Affiliated Hospital of Guizhou Medical University. Written informed consent was obtained from the patient's legal guardians.

https://doi.org/10.62347/IDNC4811

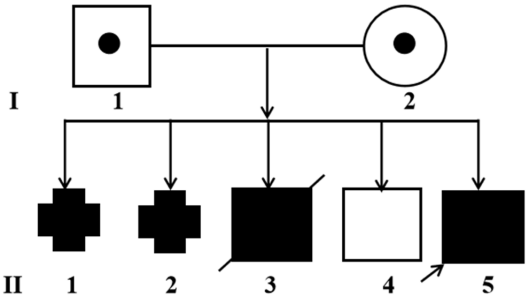

Figure 1. Family pedigree of the proband. The pedigree illustrates an autosomal recessive inheritance pattern. I-1: Father of the proband [*alkaline phosphatase-liver/bone/kidney* (*ALPL*) gene variant carrier]. I-2: Mother of the proband (*ALPL* gene variant carrier). II-1: Pregnancy 1 (G1), ended in spontaneous abortion. II-2: Pregnancy 2 (G2), terminated by induced abortion. II-3: Pregnancy 3 (G3), male fetus terminated due to severe skeletal dysplasia identified on prenatal ultrasound. II-4: Pregnancy 4 (G4), healthy male child. II-5: Pregnancy 5 (G5), the proband with infantile hypophosphatasia (HPP). Symbol definitions: □ = male; ○ = female; ● = carrier; ✚ = abortion; ■ with slash = presumed perinatal lethal HPP; big □, healthy male child; ■ with arrow, proband with confirmed infantile HPP (compound heterozygous *ALPL* mutations).

Genetic analysis

Whole-exome sequencing was performed on the proband and both parents. Variants were confirmed by Sanger sequencing and classified according to the American College of Medical Genetics and Genomics (ACMG) guidelines.

Results

Case presentation

A 1-month-old male infant (born at 33^{+6} weeks gestation by cesarean section due to premature rupture of membranes) presented with persistent oxygen dependence 47 days postpartum. Birth weight was 1,470 g, and Apgar scores were 4 and 8 at 1 and 5 minutes respectively. He required invasive mechanical ventilation (3 days) for respiratory distress syndrome and subsequent non-invasive respiratory support (16 days) for pulmonary infections.

Family history

Parents were non-consanguineous with no skeletal abnormalities. The mother (gravida 5, para 2) had a terminated pregnancy at 24^{+6} weeks due to fetal severe abnormalities (shortened long bones, narrow thorax) (Supplementary Figure 1). A subsequent full-term male sibling is healthy. Prenatal ultrasound of the proband at 31 weeks showed femur length 4 standard deviations below the mean (**Figure 1**).

Physical examination

At admission (corrected age 1 month), he had a weight 2,350 g (< 3rd percentile), length 44 cm, and head circumference 33 cm. Findings included soft cranial bones, widened fontanelles (anterior 5 × 5 cm, posterior 2 × 2 cm), shortened chest, and short extremities. Primitive reflexes were absent (Supplementary Figure 2A).

Laboratory findings

Serum alkaline phosphatase (ALP) was persistently low (1.5-12.3 U/L; normal range 34-114). Hypercalcemia was present (Ca^{2+} 2.59-5.36 mmol/L; normal 2.2-2.7). Parathyroid hormone was inappropriately normal/low (1.2-1.72 ng/mL; normal 12-65). Urinalysis revealed leukocyturia with *Escherichia coli* on culture.

Imaging

Chest X-ray showed thin ribs and a narrow chest cavity (Supplementary Figure 2C). Cranial computed tomography/magnetic resonance imaging demonstrated thin calvarial bones with ossification defects (Supplementary Figure 2B). Long bone radiographs revealed osteopenia, metaphyseal fraying, and cupping without fractures (Supplementary Figure 3). Renal ultrasound showed medullary nephrocalcinosis (Supplementary Figure 4).

Genetic testing

The patient carried two heterozygous *ALPL* variants: c.533A>G (p.Tyr178Cys) from the father and c.644T>A (p.Ile215Asn) from the mother, confirmed as compound heterozygous. Both are classified as variants of uncertain significance (VUS) per ACMG guidelines (**Figure 2**).

Clinical course

The infant developed progressive respiratory deterioration requiring high-flow nasal cannula, vitamin B6-responsive seizures, feeding intolerance with failure to thrive, and recurrent pulmonary/urinary tract infections (Supplementary

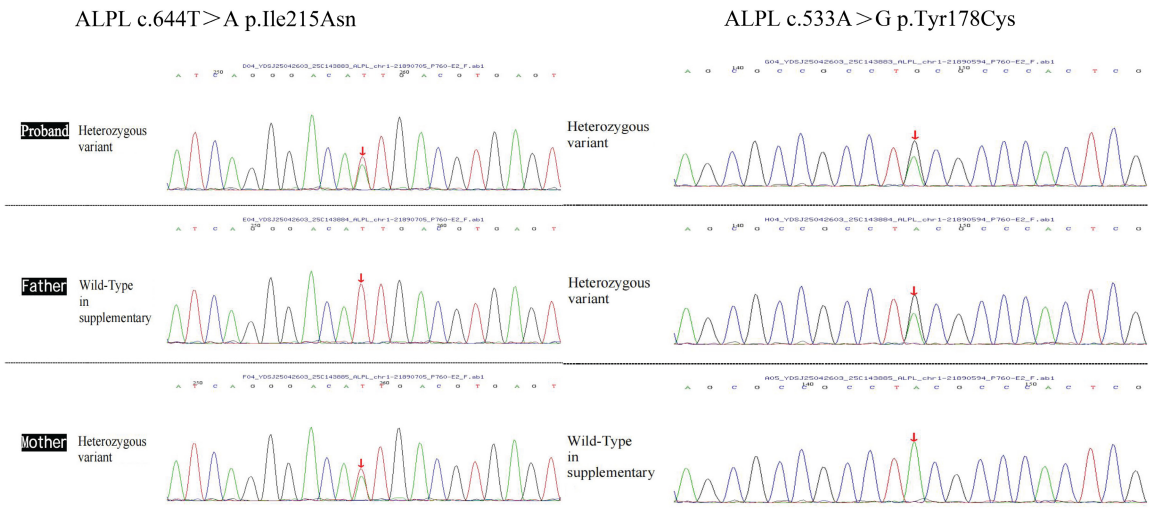

Figure 2. Whole-exome sequencing results of the proband and parents. Proband: Compound heterozygous for the *ALPL* variants c.533A>G (p.Tyr178Cys) and c.644T>A (p.Ile215Asn). Father: Heterozygous carrier of the c.533A>G (p.Tyr178Cys) variant; wild-type for c.644T>A. Mother: Heterozygous carrier of the c.644T>A (p.Ile215Asn) variant; wild-type for c.533A>G.

Figure 5A). Hypercalcemia, hypomagnesemia, and hypophosphatemia persisted. Enzyme replacement therapy (ERT) was not administered. After 133 days, the patient was discharged against medical advice. At discharge (corrected age: > 4 months), weight was 3,070 g, length 50 cm (both < 3rd percentile). Developmental milestones included social smiling and head lifting, but no rolling or sitting with support (Supplementary Figure 5B).

Discussion

This report describes an infant with severe HPP due to compound heterozygous ALPL mutations. The clinical presentation, profoundly low ALP, hypercalcemia, vitamin B6-responsive seizures, respiratory insufficiency, and skeletal demineralization, are characteristic of the infantile phenotype [4].

The two missense mutations, c.533A>G (p.Tyr178Cys) and c.644T>A (p.Ile215Asn), are located in the catalytic domain of TNSALP. The tyrosine at position 178 is involved in substrate binding; substitution with cysteine likely disrupts catalytic efficiency. The isoleucine at position 215 resides in a hydrophobic region near the metal-binding site; replacement with asparagine may affect enzyme stability. Although both variants are classified as VUS, evidence supports their pathogenicity [7, 8]. The compound heterozygous state, with each variant inherited from an unaffected carrier parent and segregation with disease in the family, supports a recessive loss-of-function mechanism. The combination of these mutations likely causes severely impaired enzyme activity, consistent with the observed severe infantile phenotype.

The mother's history of a pregnancy terminated for severe skeletal abnormalities, combined with carrier status for one variant, underscores the importance of genetic counseling in affected families. Prenatal diagnosis should be considered in subsequent pregnancies.

ERT with asfotase alfa is the only disease-modifying therapy for HPP, dramatically improving survival in severe cases. Literature review demonstrates 85.0% survival with ERT versus 29.63% without [9]. Our patient did not receive ERT, and his progressive deterioration highlights the urgent need for early treatment access.

Hypercalcemia in HPP results from increased bone resorption and renal tubular reabsorption due to impaired mineralization [10]. Nephrocalcinosis, as seen in this case, is a common complication of chronic hypercalcemia.

Limitations include lack of functional studies for the identified variants and inability to test the healthy sibling. However, the strong geno-

type-phenotype correlation supports the diagnosis.

Conclusion

Infantile HPP due to compound heterozygous ALPL mutations presents with characteristic features, including profoundly low ALP, hypercalcemia, respiratory insufficiency, and vitamin B6-responsive seizures. Early diagnosis and prompt initiation of ERT are essential to improve outcome. This case highlights the need for increased clinical awareness and access to targeted therapy.

Acknowledgements

This work was supported by 2024 Annual Guizhou Province Health and Wellness High-Quality Development Medical Research Joint Fund Project (2024GZYXKYJJXM0064).

Disclosure of conflict of interest

None.

Address correspondence to: Maoqiong Chen, Department of Neonatology, Affiliated Hospital of Guizhou Medical University/Guizhou Hospital, First Affiliated Hospital of Sun Yat-Sen University, Guiyang 550000, Guizhou, China. Tel: +86-88689207; E-mail: chenmaoqiong189@163.com

References

[1] Im M and Cho SY. Hypophosphatasia in childhood: diagnosis to management. Osteoporos Sarcopenia 2025; 11: 38-42.
[2] Seefried L, Genest F, Hofmann C, Brandi ML and Rush E. Diagnosis and treatment of hypophosphatasia. Calcif Tissue Int 2025; 116: 46.
[3] Okawa R and Nakano K. Dental manifestation and management of hypophosphatasia. Jpn Dent Sci Rev 2022; 58: 208-216.
[4] Hogler W, Montero-Lopez R, Farman MR, Hogler F, Saraff V and Hogler W. Challenges in hypophosphatasia: suspicion, diagnosis, genetics, management, and follow-up. Horm Res Paediatr 2025; 98: 736-745.
[5] Whyte MP, McAlister WH, Mack KE, Mumm S and Madson KL. Pediatric hypophosphatasia: avoid diagnosis missteps! J Bone Miner Res 2024; 39: 655-660.
[6] Cerar S, Paro-Panjan D and Soltirovska-Salamon A. The role of quantitative ultrasound in diagnosing severe bone metabolic diseases in newborns. Front Pediatr 2023; 11: 1109553.
[7] Farman MR, Rehder C, Malli T, Rockman-Greenberg C, Dahir K, Martos-Moreno GA, Linglart A, Ozono K, Seefried L, Del Angel G, Webersinke G, Barbazza F, John LK, Delana Mudiyanselage SMA, Hogler F, Nading EB, Huggins E, Rush ET, El-Gazzar A, Kishnani PS and Hogler W. The global ALPL gene variant classification project: dedicated to deciphering variants. Bone 2024; 178: 116947.
[8] Mornet E, Taillandier A, Domingues C, Dufour A, Benaloun E, Lavaud N, Wallon F, Rousseau N, Charle C, Guberto M, Muti C and Simon-Bouy B. Hypophosphatasia: a genetic-based nosology and new insights in genotype-phenotype correlation. Eur J Hum Genet 2021; 29: 289-299.
[9] Dahir KM, Shannon A, Dunn D, Voegtli W, Dong Q, Hasan J, Pradhan R, Pelto R and Pan WJ. Safety, pharmacokinetics, and pharmacodynamics of efzimfotase alfa, a second-generation enzyme replacement therapy: phase 1, dose-escalation study in adults with hypophosphatasia. J Bone Miner Res 2024; 39: 1412-1423.
[10] Fenn JS, Lorde N, Ward JM and Borovickova I. Hypophosphatasia. J Clin Pathol 2021; 74: 635-640.

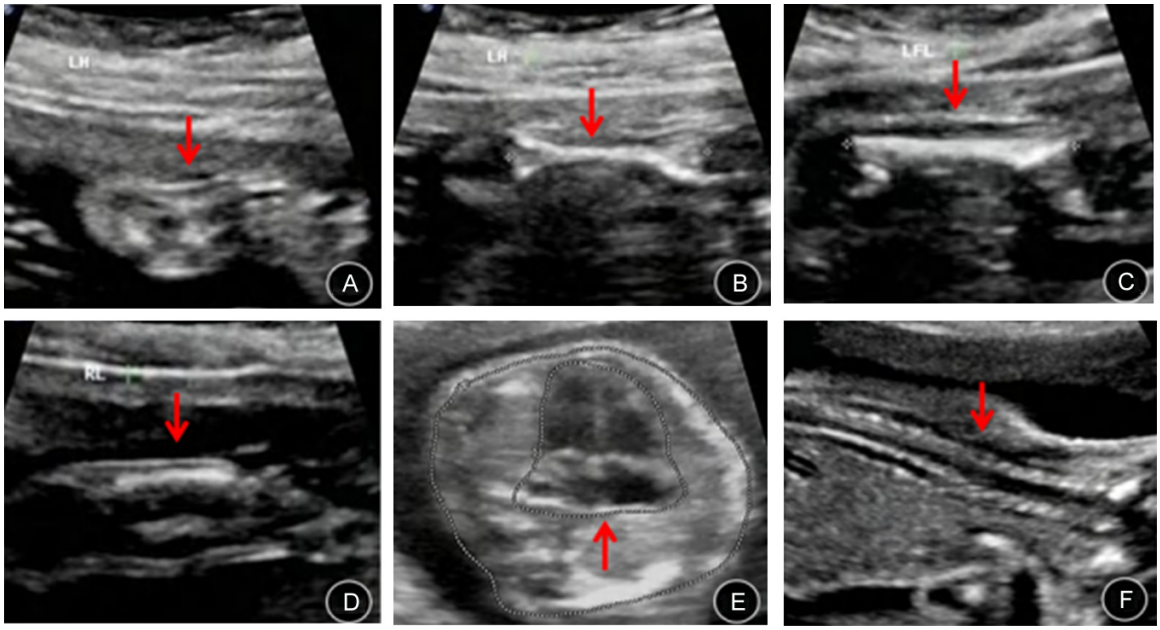

Supplementary Figure 1. Prenatal ultrasound images of the G3 fetus at 24 weeks of gestation. (A-F) Sequential images demonstrating markedly shortened long bones, corresponding to the ulna and radius (A), humerus (B), femur (C), tibia and fibula (D), fetal skull (E), and fetal thorax (F). The findings are consistent with severe skeletal dysplasia, characterized by shortened limbs and posterior acoustic shadowing.

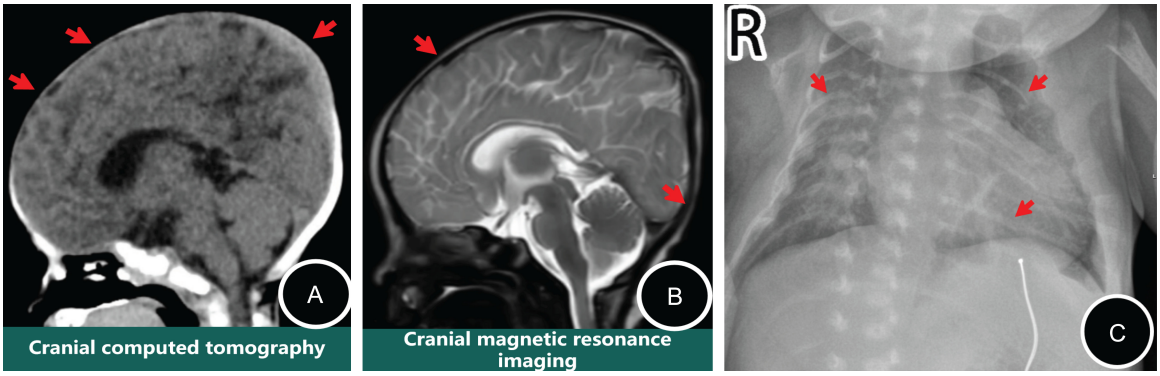

Supplementary Figure 2. Imaging findings demonstrating skeletal pathology. A. Cranial computed tomography, sagittal view. B. Cranial magnetic resonance imaging, sagittal view. Both images reveal diffuse thinning of the cranial bone cortex, markedly reduced bone density, localized comminuted bone fragments, and multiple cranial ossification defects. C. Chest radiograph, anterior-posterior view, showing slender, gracile ribs, and retraction of the chest wall (indicated by the red arrow), consistent with a hypoplastic thorax.

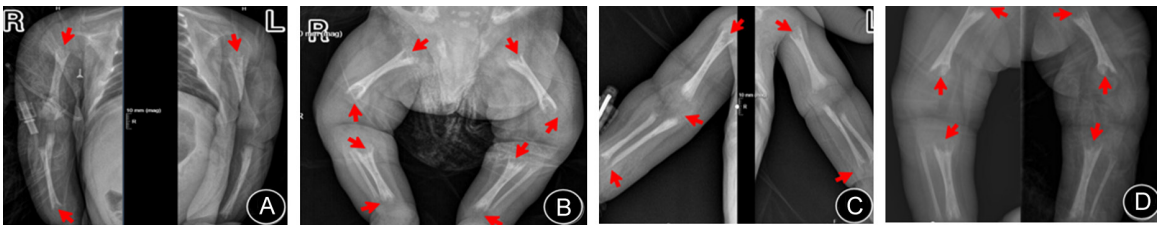

Supplementary Figure 3. Serial radiographic progression of long bones in the limbs. A and B. Anteroposterior radiographs of the upper and lower limb long bones, respectively, obtained at 2 months of age. C and D. Corresponding anteroposterior views taken at 4 months of age. The images demonstrate progressive osteopenia, cortical thinning, obliteration of the provisional calcification zones, and characteristic metaphyseal fraying and cupping (indicated by red arrows).

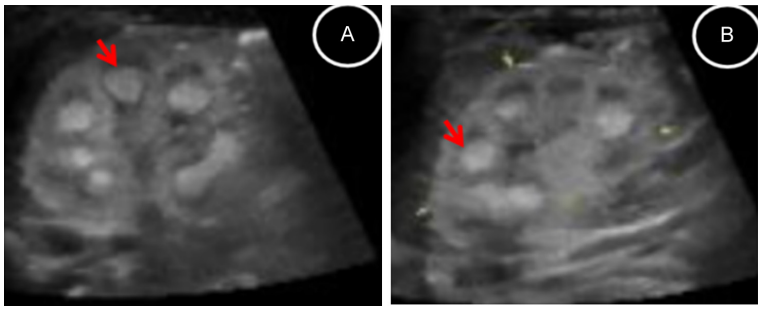

Supplementary Figure 4. Renal ultrasound images demonstrating medullary calcifications. The images (A) and (B) present ultrasound images of the left and right kidney, respectively. Bilateral renal medullary calcifications are evident, exhibiting a characteristic petal-like distribution (indicated by red arrows).

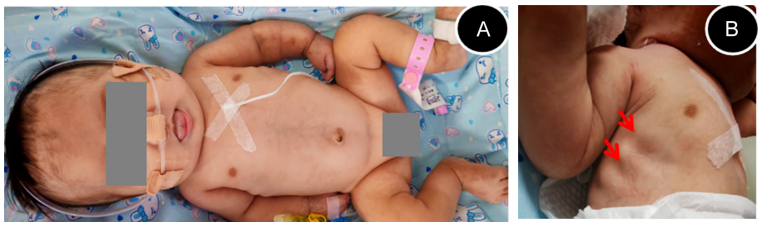

Supplementary Figure 5. Clinical photographs of the patient on admission and before discharge. A. Appearance on admission, demonstrating shortened extremities. B. Appearance at the time of discharge, showing the characteristic finding of rachitic rosary (beaded ribs, indicated by red arrow).